ENVIRONMENTAL RESEARCH
INFRASTRUCTURE AND SUSTAINABILITY

PURPOSE-LED PUBLISHING™

Part of the ENVIRONMENTAL RESEARCH SERIES

LETTER • OPEN ACCESS

Urban green space metric choice and weighting matter for assessing cooling benefits for human health

To cite this article: Armande Aboudrar-Méda and Giacomo Falchetta 2026 *Environ. Res.: Infrastruct. Sustain.* **6** 021001

ENVIRONMENTAL RESEARCH
INFRASTRUCTURE AND SUSTAINABILITY

OPEN ACCESS

RECEIVED
19 March 2026

REVISED
28 April 2026

ACCEPTED FOR PUBLICATION
1 June 2026

PUBLISHED
10 June 2026

LETTER

Urban green space metric choice and weighting matter for assessing cooling benefits for human health

Armande Aboudrar-Méda[1] **and Giacomo Falchetta**[1,2,*]

[1] Fondazione Centro Euro-Mediterraneo sui Cambiamenti Climatici, RFF-CMCC European Institute on Economics and the Environment, Venice, Italy
[2] International Institute for Applied Systems Analysis, Schlossplatz, 1, Laxenburg A-2361, Austria
[*] Author to whom any correspondence should be addressed.

E-mail: giacomo.falchetta@cmcc.it

Keywords: urban green space, heat-related mortality, climate adaptation, metric choice, spatial weighting

Supplementary material for this article is available online

Abstract

Extreme heat is a growing source of health-related risk in cities, and urban greening is widely promoted as a strategy to reduce its adverse consequences. However, urban green space can be measured in very different ways, and it remains unclear whether commonly used metrics are interchangeable when estimating health-relevant cooling benefits. Here we test how green space metric choice affects inferred heat-mortality attenuation in Paris using a harmonised arrondissement-day panel for the 2008–2017 summer seasons, combining daily mortality, 100-meter resolution UrbClim heat fields, and three urban vegetation measurement approaches: street-level green view index (GVI), satellite-derived normalized difference vegetation index (NDVI), and local planimetry-based vegetation cover (IMU). We estimate conditional time-series distributed lag non-linear models across nine heat indicators. Greener arrondissements consistently show lower heat-related mortality risk: across all 45 heat-metric and greenness-metric combinations assessed. Street-level GVI yields the strongest central attenuation estimate, followed closely by NDVI, and finally by IMU. For example, for mean daily wet-bulb globe temperature, the central estimate for the attenuation in heat-related mortality risk is 18.5% with GVI, compared with 16% for NDVI and 14% for planimetry-based vegetation. Despite uncertainty around individual effect sizes, the consistent directional ordering across all three metrics suggests that green-space indicators are not interchangeable in heat-health research. Metric and weighting choices made upstream—in how vegetation is measured and spatially aggregated—can materially alter estimated health burdens and, in some cases, even reverse their sign, with direct consequences for policy recommendations. We treat these findings as hypothesis-generating: more systematic investigation across cities and climate contexts is needed to establish which representations of urban greenness best capture heat-relevant cooling benefits.

1. Introduction and background

Extreme heat is a major environmental health risk in cities, and its burden is expected to increase as climate change increases its frequency, intensity, and duration. Urban populations are particularly exposed because dense built surfaces store and re-radiate heat, creating urban heat islands that elevate ambient temperatures relative to surrounding areas. This matters not only for thermal comfort, but also for mortality and morbidity, with substantial health and economic consequences across cities worldwide [1, 2]. In this context, urban greening is often highlighted as an attractive adaptation strategy, because vegetation can reduce near-surface temperatures and heat stress through shading, evapotranspiration, and changes in surface energy balance [3, 4]. A growing epidemiological and health-impact-assessment literature suggests that greener urban environments can attenuate heat-related health risks, including mortality, although the magnitude and consistency of these benefits vary across places and study designs

[5–13], with potentially reversed benefits on cold-related mortality [14]. Yet, related work has also shown greening alone is unlikely to fully offset extreme heat-health risks and should be considered alongside broader adaptation planning [13, 15–18]. Moreover, the literature increasingly points to heterogeneity in cooling and health benefits across urban form, population groups, and environmental contexts [4, 8, 17, 19]. Reviews and modelling studies further reinforce the potential of green interventions, but also the need for careful evaluation of their health relevance across intervention types, spatial contexts, and future climates [19, 20].

Despite this progress, an important knowledge gap remains in how urban green space is measured when assessing heat-health benefits. Many studies rely on remotely-sensed multispectral green space metrics, such as the normalized difference vegetation index (NDVI) or on land-cover fractions, while fewer studies use street-level or pedestrian-level indicators—such as the green view index (GVI) derived from street-view imagery or local planimetry—that may better reflect what people actually experience in the pedestrian environment [10, 11]. Those are harder to obtain for large geographical areas or samples of cities. While to some extent correlated, green space availability and density metrics are not conceptually interchangeable: they capture different dimensions of urban vegetation, from areal extent to vertical structure, visibility, and shading potential. As a result, the inferred relationship between green space and heat-health outcomes may depend not only on the presence of vegetation, but on the metric chosen to represent it. This is a critical issue because preliminary evidence already pointed towards the role of different vegetation forms and exposure definitions in yielding different estimates of heat-health protection [11]. However, such evidence remains fragmented and studies rarely focus explicitly on the consequences of metric choice itself for estimating cooling benefits relevant to human health.

Here we examine whether and how the choice of urban green space metric affects the assessment of cooling benefits for human health. Specifically, we compare three alternative green space metrics that capture different dimensions of urban vegetation: (1) official planimetry maps of high and low vegetation-covered surface (*IMU - Îlots morphologiques urbains d'Île-de-France*); (2) the GVI, a metric capturing pedestrian-level canopy cover [21]; and (3) the NDVI [22], a remotely sensed multispectral metric of greenness, widely used to proxy the density and health of vegetation. In our study, we evaluate how these alternative representations of urban-scale vegetation shape estimated statistical associations between greenness, urban cooling, and heat-health relevance in the city of Paris. To characterise the spatio-temporal variability in the heat load within the city of Paris, we rely on 100-meter resolution urban microclimate model outputs for nine different heat-related metrics (daily maximum, mean, and minimum 2m air temperature (T2M), wet-bulb globe temperature (WBGT) and land surface temperature (LST)). By doing so, we aim to clarify whether different metrics lead to systematically different conclusions about the magnitude, spatial pattern, and policy relevance of urban greening benefits and how this varies across different urban forms within a city. Ultimately, our findings provide guidance on selecting green space indicators that are most appropriate for heat-health assessments.

Building on previous evidence, and chiefly Achebak *et al* [13], our contribution is not to claim a statistically established superiority of one green space metric over the others, but to test whether a harmonised comparison yields a stable directional ordering across metrics. We show that estimated heat-related mortality attenuation is generally larger for minimum than for maximum values of daily heat metrics and that, within this design, street-based canopy metrics tend to yield more protective central estimates than planimetry-derived or remotely sensed green-space metrics. We also show that population-weighting in the derivation of small-area summaries of both heat and greenness is consequential for the resulting estimates and should be treated as part of the substantive modelling design rather than a technical afterthought.

Our results therefore contribute to the literature on the effectiveness and limits of urban greening as a climate adaptation strategy by clarifying how indicator construction choices shape inference. The main implication is that metric selection and weighting are analytically meaningful decisions, even when the underlying statistical evidence remains too imprecise to support strong claims about differences in effect size.

2. Methods

2.1. Data: sources and processing

We conduct a multi-metric extension of the Paris heat–mortality conditional time-series framework [13] to test whether green space metric choice changes the estimated heat-risk attenuation under a harmonised comparison design. The unit of analysis is arrondissement-day in Paris (20 arrondissements), which is the finest spatial resolution available in the daily mortality data used here (CépiDc/Inserm; with

Table 1. Input data sources. Spatial resolution refers to the native product; all greenness and heat metrics are aggregated to arrondissement level using population-weighted (GHS-POP) or area-weighted averaging before entering the regression. IMU polygons in Paris (after spatial intersection with arrondissement boundaries): $N = 7080$; mean area $= 11\,602\ m^2$, median $= 6{,}484\ m^2$, range 300–434,307 m^2. JJAS = June–September.

Domain	Dataset	Spatial resolution	Temporal coverage	Role
Mortality	Daily all-cause deaths by arrondissement of residence (CépiDc/INSERM)	Arrondissement (N = 20)	Daily; 2008–2017 (JJAS)	Outcome
Heat	UrbClim urban climate model (VITO) [25]: T2M, WBGT, LST (min/mean/max)	100 m raster	Hourly → daily; 2008–2017	Treatment
Street-view greenness	Green view index (GVI) [24]: pedestrian-level canopy visibility (0%–100%)	Point-level (10 m spacing along street network)	Multi-epoch street-view imagery, 2016–2023 average	Effect modifier
Satellite greenness	ESA WorldCover Sentinel-2 NDVI [22]: annual peak-greenness (p90) composites	10 m raster	2020–2021 (two annual composites, pixel-averaged)	Effect modifier
Planimetry-based greenness	IMU (*Îlots morphologiques urbains*, IPR): high, low, and total vegetation fractions per urban-island polygon	Irregular polygons (see caption)	2022 vintage	Effect modifier
Population	GHS-POP 2023 [23]	100 m raster	2020 epoch	Harmonised weighting

no sub-arrondissement geocoding available). Paris is one of Europe's densest capitals and a relevant heat-risk setting: in our panel, the population-weighted JJAS mean $T2M_{mean}$ is 21.1 °C, and the p99 of daily $T2M_{max}$ reaches 35.5 °C. Daily all-cause mortality by arrondissement of residence is expanded to a complete arrondissement-day panel for 2008–2017 and restricted to June–September (JJAS), yielding 24 400 observations (table 1).

Heat metrics are derived from UrbClim 100 m outputs and aggregated to arrondissement-day using a population-weighted spatial averaging approach with a common GHS-POP population layer [23]. We analyse nine heat metrics: T2M (min/mean/max), LST (min/mean/max), and WBGT (min/mean/max). This population-weighted spatial averaging of gridded microclimate model outputs captures within-city variation in heat exposure at sub-arrondissement resolution, ensuring that the heat metric assigned to each district reflects the thermal environment experienced by its resident population. Unweighted arrondissement heat aggregation using area-weighted and IMU-level population-weighted spatial aggregation are also calculated for comparative purposes.

For urban green space measurement, we compute three different types of arrondissement-level population-weighted metrics harmonised with the same population layer (GHS-POP) used for heat metrics spatial extraction. First, we use official planimetry maps from the *IMU – Îlots morphologiques urbains d'Île-de-France*. IMU is a comprehensive urban morphology layer that partitions urban land into contiguous polygons, including not only public parks and green infrastructure but also private gardens, courtyards, street-tree alignments, and institutional grounds. Each polygon reports 'high vegetation' (`iv_haute`, tree canopy and tall shrubs) and 'low vegetation' (`iv_basse`, herbaceous cover and low shrubs); 'IMU total' is their sum. Secondly, we leverage estimates of the GVI [21, 24], a metric capturing pedestrian-level canopy cover as a fraction of the visible panorama (0%–100%). Thirdly, we use the NDVI from ESA WorldCover Sentinel-2 NDVI at 10 m resolution, using annual peak-greenness (p90) composites for 2020 and 2021 averaged at pixel level before arrondissement aggregation [22], as a remotely sensed multispectral proxy of vegetation presence and condition.

Each green space metric is population-weighted using GHS-POP in a way that is appropriate to its native spatial representation. GVI scores, available at individual street-view 10-m resolution sampling points, are aggregated as the population-weighted mean of point-level values within each arrondissement, where weights reflect the GHS-POP density at each point location. NDVI, available as a 10m raster, is spatially aggregated using `exact_extract` with GHS-POP (100-m) as the weighting surface. IMU vegetation fractions, defined over irregular urban-island polygons, are aggregated by computing the GHS-POP mass within each polygon and taking the population-weighted mean across polygons within each arrondissement. Heat metrics from UrbClim (100-m raster) are aggregated using

Figure 1. Maps of GHS-population-weighted of (a) green view index (GVI); (b) NDVI; (c) planimetry-derived green spaces availability; and (d) average daily maximum WBGT over the 2008–2017 JJAS period for each arrondissement of Paris.

Table 2. Descriptive distributions of key heat and green space metrics across the JJAS analysis panel.

Metric	Min	p10	Median	p90	Max	IQR
Daily deaths (arr.-day)	0	0	1	4	13	3
Daily deaths (city-wide)	15	27	35	43	61	9
T2M mean (°C)	11.72	16.78	20.75	25.99	33.64	4.97
LST max (°C)	15.30	24.17	32.07	42.44	55.66	10.36
WBGT mean (°C)	9.97	14.05	17.48	21.61	26.54	4.10
GVI point pop-w. (GHS)	5.52	7.09	11.44	14.81	15.85	3.55
NDVI pop-w. (GHS)	0.089	0.141	0.230	0.319	0.326	0.119
IMU total pop-w. (GHS, %)	1.80	6.43	15.14	23.08	23.74	11.75
IMU high pop-w. (GHS, %)	1.18	3.22	10.23	14.72	15.13	7.55

the same `exact_extract` approach as NDVI. This design preserves each metric's native information support while ensuring that all arrondissement-level summaries reflect population-weighted exposure rather than area-weighted averages. The resulting extracted variables are street-level greenery (`gvi_popw_points`), satellite-derived greenery (`ndvi_popw_ghs`), and planimetry-based IMU vegetation (`imu_veg_total_popw_ghs`, `imu_high_popw_ghs`, `imu_low_popw_ghs`), differentiated by high and low-level vegetation. Unweighted greenness variants are retained for sensitivity analyses, reported in the appendix. Figure 1 provides a visual representation of arrondissement-level distribution in the three resulting population-weighted green space metrics considered in our analysis and of the average daily maximum WBGT over the 2008–2017 JJAS period. Although outcomes are only observed at arrondissement level, this population-weighted extraction partially captures sub-arrondissement heterogeneity in heat and greenness exposure assignment.

The final CTS panel includes 24 400 arrondissement-day observations (20 arrondissements, JJAS 2008–2017) and 43 146 death occurrences. Table 2 reports descriptive statistics for the resulting dataset.

2.2. Statistical framework

All analyses are conducted in R. The main packages used are `gnm` [26] for conditional quasi-Poisson regression, `dlnm` [27] for distributed lag non-linear modelling, `data.Table` for data manipulation, `sf` and `terra` for spatial operations, and `exactextractr` for population-weighted raster extraction. Throughout this section, function names refer to these packages.

We estimate a conditional case time-series distributed lag non-linear model (DLNM) with quasi-Poisson likelihood. This model estimates how daily mortality risk changes as heat rises above a reference level (the minimum-mortality temperature, MMT), after controlling for seasonal timing, day-of-week, and all time-invariant arrondissement characteristics through the conditional time-series design. For each heat metric h, daily all-cause deaths Y_{it} in arrondissement i on day t are modeled as:

$$Y_{it} \sim \text{quasi-Poisson}\left(\mu_{it}\right), \quad \log \mu_{it} = \alpha_{s(i,t)} + \gamma_{\text{dow}(t)} + ns\left(\text{day\_of\_season}_t, 4\right) \times \text{year}_t + cb_h\left(H_{it}\right) + cb_h\left(H_{it}\right) \times G_i^{(m)}. \tag{1}$$

Here, $\alpha_{s(i,t)}$ denotes arrondissement–year–month strata, implemented in the `gnm` via `eliminate = stratum_f`, and $\gamma_{\text{dow}(t)}$ captures day-of-week effects. Intra-seasonal variation is controlled using $ns(\text{day\_of\_season}, 4) \times \text{year}$. The heat term $cb_h(H_{it})$ is specified as a lag 0–1 cross-basis using `crossbasis` from `dlnm`, with a natural spline in exposure including one internal knot at the metric-specific $p90$, and an integer lag basis. This lag window (same day + next day) follows the Paris CTS framework of Achebak *et al* [13] and is consistent with the predominantly acute nature of summer heat-mortality effects. We keep the lag structure fixed across all model specifications to preserve cross-metric comparability; extending lags (e.g. 0–3 or 0–7) is a possible direction for future sensitivity analysis. The interaction term between the heat cross-basis and green space metric $cb_h(H_{it}) \times G_i^{(m)}$ tests whether this heat–mortality curve is steeper or flatter in greener versus less-green arrondissements. A negative effect modification estimate indicates attenuation: for the same heat level, greener arrondissements experience a smaller relative increase in mortality risk.

Green space metrics are standardised as:

$$G_{i,\text{std}}^{(m)} = \frac{G_i^{(m)} - \text{median}\left(G^{(m)}\right)}{\text{IQR}\left(G^{(m)}\right)}. \tag{2}$$

Because greenness is treated as a time-invariant spatial characteristic over the mortality panel, these estimates capture cross-sectional effect modification of acute heat risk, not the causal impact of temporal greening interventions.

Primary results are reported as p10→p90 greenness contrasts evaluated at each heat metric's $p99$; secondary results use observed min→max contrasts. We also report Benjamini–Hochberg (BH)-adjusted q-values across the primary heat×greenness comparisons. Standard errors are based on quasi-Poisson variance scaling, with estimated dispersion $\hat{\varphi} \approx 1.005$. Residual within-stratum autocorrelation is negligible, with a median lag-1 ACF of deviance residuals of -0.046 across 7200 strata, supporting the adequacy of model-based inference.

3. Results

3.1. Heterogeneous heat-related mortality attenuation effects of green space metrics

We begin by estimating baseline heat-only models (without the modifying effect of green space indicators), which show positive excess risk at p99 versus metric-specific MMT for all nine heat metrics (appendix), ranging from +15.98% (LST max) to +22.84% (T2M mean). For T2M, baseline excess risks are +22.84% (mean), +21.52% (min), and +22.39% (max), close to the estimates of [13]. The combination of nine heat metrics × three (five, when accounting for the differentiation between total, high, and low vegetation in the IMU planimetry-derived dataset) harmonised green space metrics yields 45 combinations and corresponding regression models. For readability, the main text focuses on three representative heat endpoints spanning the three families: WBGT mean (composite thermal stress), T2M mean (air temperature), and LST max (surface temperature). Full results for all nine heat metrics are provided in the appendix.

Figure 2 shows the estimated exposure–response curves by greenness level. On the y-axis, Relative Risk (RR) is the ratio of expected mortality at a given heat level relative to expected mortality at that metric's MMT ($RR = 1$ indicates no excess risk). Solid curves represent lower greenness (p10) and

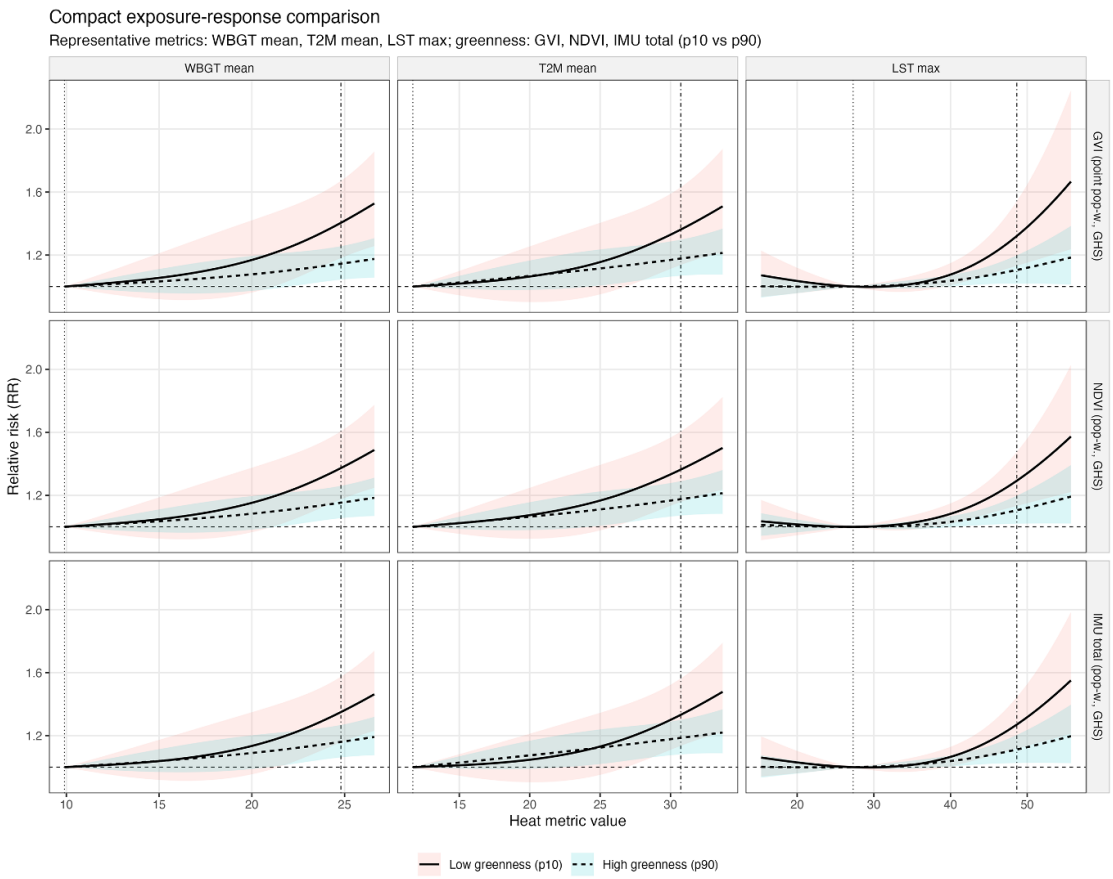

Figure 2. Exposure–response curves for Paris summer (JJAS, 2008–2017) for the representative heat endpoints (WBGT mean, T2M mean, LST max). Columns correspond to heat metrics; rows to green space metrics. RR on the *y*-axis is evaluated relative to each heat metric's MMT ($RR = 1$: no excess risk). Solid red lines indicate low greenness (p10), dashed blue lines high greenness (p90), and shaded ribbons 95% confidence intervals; vertical reference lines indicate MMT and p99. The visual gap between curves shows estimated attenuation: where the dashed curve lies below the solid curve, greenness is associated with lower heat-related mortality risk. Quantitative results for the three representative heat endpoints (WBGT mean, T2M mean, LST max) are reported in table 3.

Table 3. Selected effect-modification estimates (% change in RR at p99).

Heat metric	Green metric	Primary (p10→p90)	Secondary (min→max)
WBGT mean	GVI (point pop-w., GHS)	–18.49 (–34.78, 1.87)	–23.94 (–43.57, 2.52)
WBGT mean	NDVI (pop-w., GHS)	–16.02 (–31.20, 2.50)	–20.77 (–39.26, 3.35)
WBGT mean	IMU total (pop-w., GHS)	–14.03 (–29.26, 4.49)	–18.05 (–36.63, 5.96)
T2M mean	GVI (point pop-w., GHS)	–13.52 (–31.46, 9.12)	–17.67 (–39.69, 12.40)
T2M mean	NDVI (pop-w., GHS)	–13.77 (–29.93, 6.12)	–17.92 (–37.76, 8.24)
T2M mean	IMU total (pop-w., GHS)	–10.99 (–27.35, 9.06)	–14.22 (–34.36, 12.10)
LST max	GVI (point pop-w., GHS)	–16.34 (–31.20, 1.73)	–21.25 (–39.39, 2.32)
LST max	NDVI (pop-w., GHS)	–14.51 (–27.86, 1.31)	–18.86 (–35.31, 1.76)
LST max	IMU total (pop-w., GHS)	–12.48 (–25.81, 3.24)	–16.11 (–32.52, 4.29)

dashed curves higher greenness (p90); when the dashed curve lies below the solid curve, greenness attenuates heat-related risk. Shaded bands are 95% confidence intervals, and vertical reference lines indicate MMT and p99.

Table 3 reports the three representative heat endpoints. All central p10→p90 estimates are protective (negative), though uncertainty remains wide. For $WBGT_{mean}$, central attenuation is GVI −18.49% (95% CI: −34.78, 1.87), NDVI −16.02% (95% CI: −31.20, 2.50), and IMU total −14.03% (95% CI: −29.26, 4.49). For $T2M_{mean}$: −13.52%, −13.77%, and −10.99%, respectively. For LST_{max}: −16.34%, −14.51%, and −12.48%, respectively. Across these representative endpoints, all central estimates are protective, but the exact ordering between GVI and NDVI is not identical: GVI is more protective for $WBGT_{mean}$ and LST_{max}, while NDVI is slightly more protective for $T2M_{mean}$. IMU total is weakest in all three. Across the full nine-metric set (appendix), only $WBGT_{min}$ ×GVI excludes 0 at the 95% level.

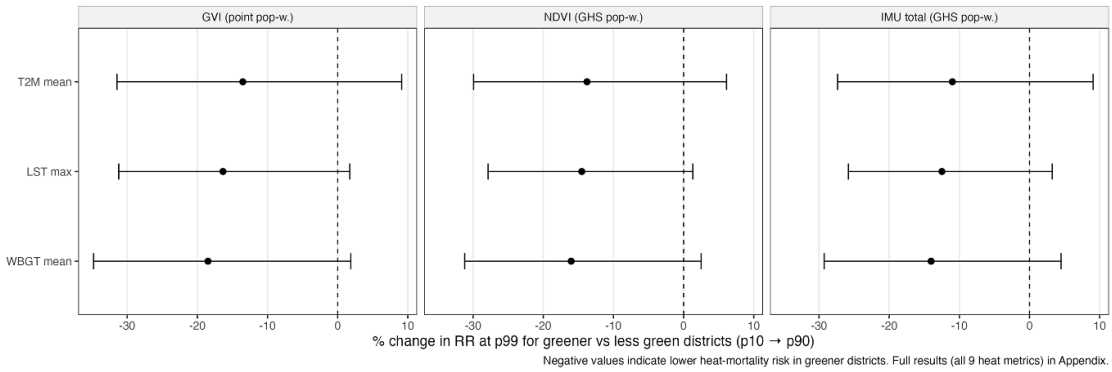

Figure 3. Forest plot of effect-modification estimates at p99 for the three representative heat endpoints (WBGT mean, T2M mean, LST max) and three green space metrics (GVI, NDVI, IMU total). Each dot is the estimated percentage change in relative risk at p99 when greenness moves from the 10th to the 90th percentile; horizontal lines are 95% confidence intervals. Negative values indicate that greener arrondissements experience lower heat-related mortality risk. The vertical dashed line at zero indicates no effect modification. Full results for all nine heat metrics are reported in the appendix.

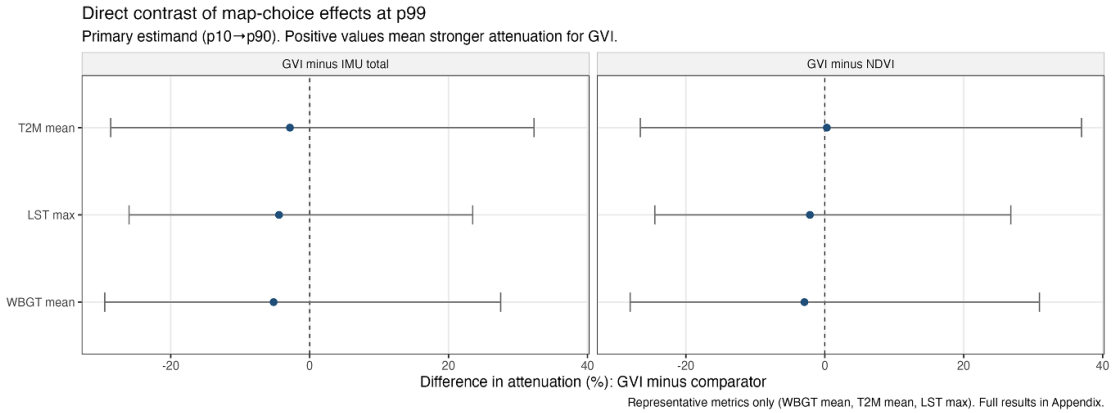

Figure 4. Direct contrasts at p99 (primary p10→p90 estimand). Left panel: GVI minus IMU total; right panel: GVI minus NDVI. Each row is one heat metric; dots are point estimates and horizontal lines are 95% confidence intervals. Positive values indicate stronger estimated attenuation for GVI; the vertical dashed line at 0 indicates no between-metric difference. Full results for all nine heat metrics in appendix.

Secondary min→max contrasts are larger in absolute value and preserve the same ranking pattern for these three representative heat endpoints. Figure 3 summarises these estimates as a forest plot. To assess between-metric separation under the primary p10→p90 estimand, figure 4 reports direct pairwise contrasts (GVI minus NDVI; GVI minus IMU total): for the representative trio, contrasts are small in absolute magnitude (about 0.3%–5.2% points) and all 95% confidence intervals include zero. Full nine-metric secondary results are provided in the appendix.

Attributable-burden scenarios (per 100 000 residents per JJAS season; denominator 2.2 million over 10 summers), reported in table 4, differ by metric and can change sign depending on the heat–greenness pair. Under WBGT mean (MMT), avoided burden in the max-all scenario was 4.25 for GVI, 2.47 for NDVI, and 1.47 for IMU total. Under T2M mean at MMT, GVI (0.87) and NDVI (1.42) remained positive, while IMU total (−0.66) turned negative. Under LST max (MMT), values are 1.29 (GVI), 1.40 (NDVI), and 0.73 (IMU total). We note that the sign reversal for IMU total under T2M arises in scenario calculations when the estimated exposure-response curve is shallow or unstable near the chosen threshold and the greenness interaction is imprecisely estimated, so small differences in the curve around the MMT can change the sign of the integrated attributable burden. Figure 5 visualises these burden comparisons across the three heat endpoints and green space metrics.

The wide confidence intervals are a direct consequence of the identification structure. Greenness is a time-invariant, district-level characteristic, so the interaction between the heat cross-basis and greenness is identified exclusively from cross-sectional variation across the 20 arrondissements. The conditional time-series design efficiently absorbs temporal confounders through arrondissement–year–month

Table 4. Attributable-burden scenario comparison (avoided deaths per 100 000 residents per JJAS season), symmetric 3×3 design, all MMT threshold.

Heat	Green metric	Threshold	Obs. burden	Avoided max-all	% red.	Avoided p90-floor	Avoided + 1IQR-cap
WBGT mean	GVI (point pop-w., GHS)	MMT	13.48	4.25	31.5	2.98	3.22
WBGT mean	NDVI (pop-w., GHS)	MMT	13.56	2.47	18.2	2.20	2.22
WBGT mean	IMU total (pop-w., GHS)	MMT	13.53	1.47	10.8	1.31	1.34
T2M mean	GVI (point pop-w., GHS)	MMT	14.86	0.87	5.9	0.62	0.66
T2M mean	NDVI (pop-w., GHS)	MMT	14.93	1.42	9.5	1.27	1.28
T2M mean	IMU total (pop-w., GHS)	MMT	14.88	−0.66	−4.4	−0.58	−0.60
LST max	GVI (point pop-w., GHS)	MMT	4.16	1.29	31.0	0.90	0.98
LST max	NDVI (pop-w., GHS)	MMT	4.13	1.40	34.0	1.26	1.27
LST max	IMU total (pop-w., GHS)	MMT	4.14	0.73	17.6	0.65	0.66

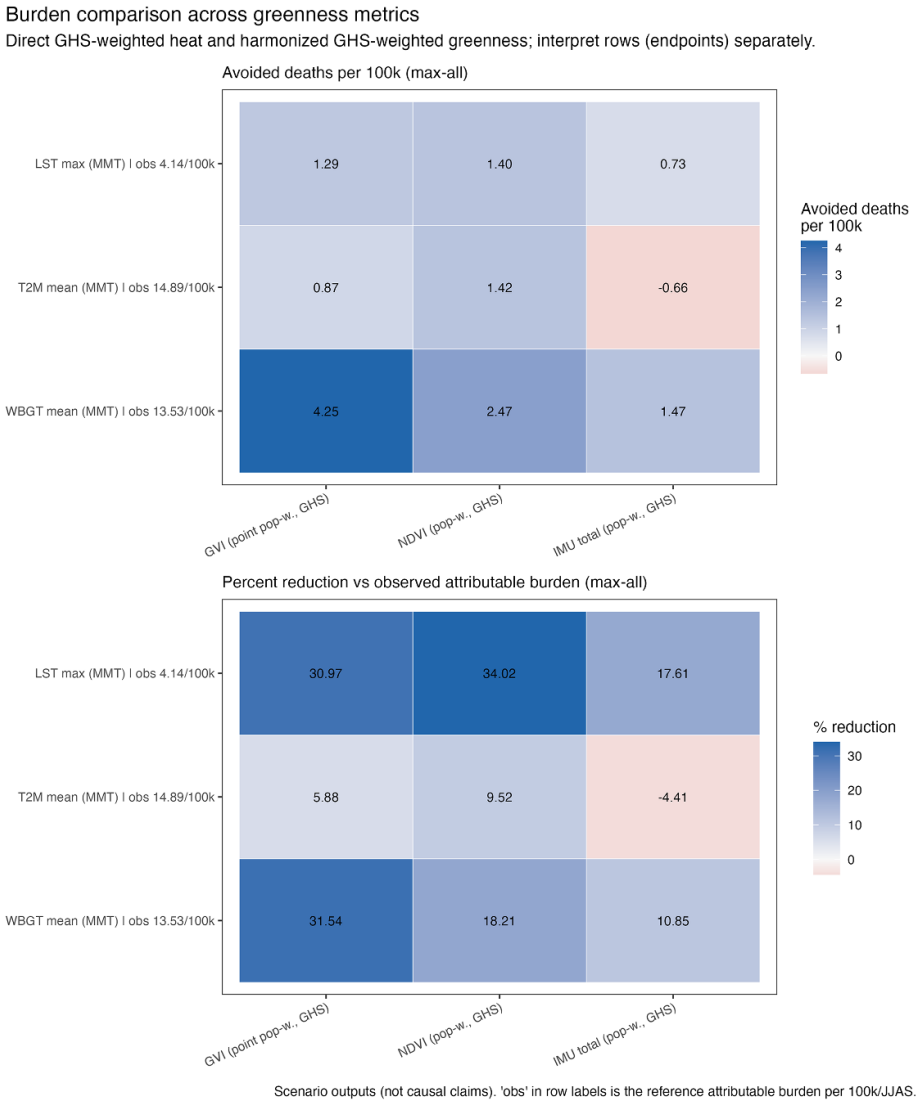

Figure 5. Scenario burden comparison across key heat endpoints and green space metrics (max-all scenario). Top panel shows avoided deaths per 100 000 per JJAS season; bottom panel shows percent reduction versus observed attributable burden. Read rows (heat endpoints) separately and compare columns (green space metrics). Positive values indicate avoided burden; negative values indicate unstable scenario estimates under weak signal conditions.

strata, but this same conditioning means that the effective sample size for the spatial modifier is $N = 20$, regardless of the number of daily observations. Standard errors on the interaction term therefore scale with the between-district variation in greenness, which is inherently limited in a single city. Diagnostic

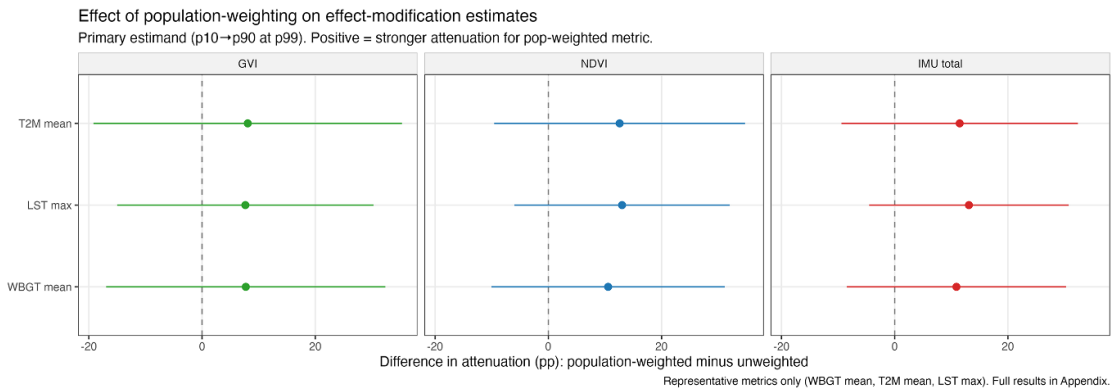

Figure 6. Effect of population-weighting on effect-modification estimates at p99 (primary p10→p90 estimand). Panels correspond to greenness families (GVI, NDVI, IMU total); rows are heat metrics. Dots are weighted-minus-unweighted differences and horizontal lines are 95% confidence intervals. Positive values indicate stronger estimated attenuation under population-weighted aggregation; 0 indicates no weighting effect. Representative metrics only; full results in appendix.

checks confirm that the quasi-Poisson model-based standard errors are adequate: the estimated dispersion parameter is close to 1 ($\hat{\varphi} \approx 1.005$) and within-stratum residual autocorrelation is negligible (median lag-1 autocorrelation of deviance residuals: −0.046), so the imprecision reflects genuine statistical power constraints rather than model misspecification. Importantly, the consistency of the protective pattern across all 45 specifications heat–greenness combinations, coupled with the stable ranking of metrics, suggests that the underlying signal is robust even if individual contrasts are imprecisely estimated. This implies limited power to detect moderate between-metric differences in effect size, so the analysis is most informative for directional consistency and ranking rather than precise pairwise separation.

3.2. Small area unit-level spatial weighting implications

Figure 6 demonstrates that population-weighting of vegetation metrics consistently strengthens estimated attenuation relative to unweighted metrics, with the effect largest for planimetry-based IMU vegetation and smallest for GVI. This pattern is consistent with metric support: NDVI and IMU are area-based surfaces, so unweighted aggregation gives equal influence to low-population land where human exposure is limited, while population-weighting recentres these metrics on where residents live. By contrast, GVI is by design street-sampled and therefore already closer to population activity spaces, so weighted-minus-unweighted shifts are smaller. Taken together, weighting should be treated as part of estimand definition rather than as a technical post-processing choice.

4. Discussion and conclusions

4.1. Implications for research and practice

Our findings suggest that estimates of the heat-health benefits of urban greening depend not only on how much vegetation is present, but also on how greenness is measured and spatially weighted. In Paris, street-level greenness captured by the GVI generally yields more protective central estimates of heat-related mortality attenuation than NDVI or planimetry-based vegetation measures, with NDVI slightly more protective for the two T2M variants; attributable-burden calculations differ accordingly. and the attributable-burden calculations differ accordingly. The primary implication is methodological: green-space indicators are not interchangeable for adaptation assessment, and metric selection plus spatial weighting should be treated as substantive modelling decisions rather than neutral data choices. Our results are best interpreted as measurement guidance, rather than intervention prescription.

Different metric–heat combinations are informative for different research or policy questions. GVI captures pedestrian-level canopy visibility and is closely aligned with street-level thermal experience; NDVI, as a temporally resolved satellite product available globally, is suited to satellite-based monitoring and temporal vegetation dynamics; and IMU provides a complete planimetry-based decomposition of urban land cover, useful for land-use and zoning analyses. On the heat side, WBGT is most directly linked to human thermal stress, T2M is the most generalisable and communicable metric, and LST captures surface thermal patterns relevant to radiant load. Across combinations, the protective direction

is highly consistent, but differences in magnitude remain imprecisely estimated. Notably, the only primary estimate excluding zero is $WBGT_{min} \times GVI$ (−23.73%, 95% CI: −39.27, −4.21), which we interpret as supportive but not definitive evidence within a broader hypothesis-generating pattern. For applied assessments, a harmonised multi-metric strategy—combining at least one street-view metric with one satellite or planimetry-based metric—is therefore preferable.

For planners and public-health practitioners, the stronger signal associated with street-level canopy measures is consistent with the relevance of pedestrian-level thermal conditions for health, but translating this into specific infrastructure recommendations requires evidence from intervention studies that our cross-sectional design cannot provide. This interpretation is consistent with recent literature emphasising that both greenness and heat metric definitions influence inferred heat-health relationships [28–30]. While individual effect sizes remain imprecisely estimated—only one of 45 primary comparisons excludes zero at the 95% level—the consistency of the directional ordering across all heat–greenness combinations suggests that the ranking is robust. This ranking should be interpreted as hypothesis-generating rather than confirmatory evidence of metric superiority, since differences in native variance, spatial support, and measurement error may also contribute. The contribution of this study lies in demonstrating that metric choice and weighting shape inference, rather than in definitive quantification of effect sizes.

4.2. Limitations and future work

Despite the practical relevance of these findings, several limitations are central rather than peripheral. First, uncertainty remains substantial: among the 45 primary heat-greenness comparisons, only one excludes zero at the 95% level, and none remain significant after multiple-testing correction. This is not surprising once the identification structure is recognized: the design identifies cross-sectional effect modification of short-term heat risk by existing greenness differences, not the causal effect of greening interventions over time. Although the panel contains 24 400 arrondissement-day observations, the greenness interaction is identified from cross-sectional variation across only 20 arrondissements. In other words, the effective sample size for the spatial modifier is $N = 20$, which fundamentally limits power to distinguish moderate differences between green space metrics. The broad tendency toward negative estimates is therefore informative, but it should not be overstated. A formal power or simulation exercise would be a useful extension for future work.

Second, the analysis is restricted to Paris and to arrondissement-level contrasts, and arrondissement is the finest spatial scale available in the mortality data. We therefore cannot estimate within-arrondissement mortality gradients directly; future work with finer geocoded mortality data (where available) would be a valuable extension. Moreover, the external validity of the findings presented in this paper remains an open question for future research.

Third, some key inputs are effectively time-invariant or available over partially overlapping periods. GVI is derived from a single-epoch street-view product, NDVI uses ESA 10 m 2020–2021 composites, and GHS-POP represents one population surface applied to the full 2008–2017 mortality panel. This is a practical and standard simplification for small-area heat-health studies, but it cannot capture temporal changes in vegetation cover, canopy growth, or population redistribution. Finally, although the harmonised weighting strategy is a strength for comparability, any spatial aggregation necessarily simplifies local heterogeneity in exposure, accessibility, and population vulnerability.

Cross-metric comparisons should also be interpreted with explicit attention to spatial support. GVI is point-sampled and pedestrian-facing, NDVI is a 10-m raster product, and IMU is polygon-based. Even if these metrics partly reflect the same underlying greenness construct, an IQR-standardised contrast does not correspond to the same real-world exposure gradient across them. Point-sampled GVI can preserve more micro-scale heterogeneity than NDVI or IMU and may therefore generate larger standardised contrasts if the exposure-response relationship is nonlinear or if fine-scale canopy structure is especially relevant for thermal experience. Differences in estimated effect sizes across metrics thus reflect both different ecological dimensions of vegetation and different measurement supports. Accordingly, differences in ranking may reflect both ecological mechanisms and measurement properties, so cross-metric ordering should be treated as hypothesis-generating evidence rather than confirmatory proof.

The attributable-burden sign reversals also merit caution. Negative avoided-burden values for some T2M mean scenarios do not imply that greening increases mortality. Rather, they arise because burden calculations integrate an estimated exposure-response curve relative to a threshold, so when that curve is shallow and uncertain around the MMT, small fluctuations in the interaction estimate can change the sign of the integral. These scenarios should therefore be interpreted as evidence of instability in burden attribution under weak signal conditions, not as evidence of harmful greenness.

To conclude, future heat-health assessments should therefore treat metric selection as a substantive analytical decision rather than a neutral data choice. Doing so should improve both the scientific robustness and the policy relevance of evidence used to design urban greening strategies under a warming climate.

Data availability statement

Restrictions apply to mortality data, which are obtained under agreement from the Epidemiology Centre on Medical Causes of Death (CépiDC) of Inserm and are therefore not publicly available. UrbClim data are publicly accessible via the VITO PROVIDE API and via the Copernicus Climate Data Store interface. NDVI data are derived from ESA WorldCover Sentinel-2 10 m products. GHS-POP data are publicly available from the Copernicus Emergency Management Service. IMU data are publicly available from Institut Paris Region (IPR): Îlots de chaleur urbains (ICU) d'Île-de-France (IAU open data). Street-level GVI input data are obtained from [24].

The data that support the findings of this study are openly available at the following URL/DOI: https://github.com/ArmandeCMCC/GVIestim [31].

Supplementary data 1 available at: https://doi.org/10.1088/2634-4505/ae75a1/data1.

Competing interests

The authors declare no competing interests.

Author contributions

Armande Aboudrar-Méda 0009-0008-0978-2412
Conceptualization (supporting), Data curation (lead), Formal analysis (lead), Investigation (equal), Methodology (equal), Resources (lead), Software (lead), Validation (lead), Visualization (lead), Writing – original draft (equal), Writing – review & editing (equal)

References

[1] Huang W T K, Masselot P, Bou-Zeid E, Fatichi S, Paschalis A, Sun T, Gasparrini A and Manoli G 2023 Economic valuation of temperature-related mortality attributed to urban heat islands in European cities *Nat. Commun.* **14** 7438
[2] Sera F *et al* 2019 How urban characteristics affect vulnerability to heat and cold: a multi-country analysis *Int. J. Epidemiol.* **48** 1101–12
[3] Santamouris M and Osmond P 2020 Increasing green infrastructure in cities: impact on ambient temperature, air quality and heat-related mortality and morbidity *Buildings* **10** 233
[4] Gillerot L, Landuyt D, De Frenne P, Muys B and Verheyen K 2024 Urban tree canopies drive human heat stress mitigation *Urban Forestry Urban Greening* **92** 128192
[5] Chen D, Wang X, Thatcher M, Barnett G, Kachenko A and Prince R 2014 Urban vegetation for reducing heat related mortality *Environ. Pollut.* **192** 275–84
[6] Burkart K, Meier F, Schneider A, Breitner S, Canário P, João Alcoforado M, Scherer D and Endlicher W 2015 Modification of heat-related mortality in an elderly urban population by vegetation (urban green) and proximity to water (urban blue): evidence from Lisbon, Portugal *Environ. Health Perspect.* **124** 927
[7] Son J-Y, Lane K J, Lee J-T and Bell M L 2016 Urban vegetation and heat-related mortality in Seoul, Korea *Environ. Res.* **151** 728–33
[8] Choi H M *et al* 2022 Effect modification of greenness on the association between heat and mortality: a multi-city multi-country study *eBioMedicine* **84** 104251
[9] Iungman T *et al* 2023 Cooling cities through urban green infrastructure: a health impact assessment of European cities *Lancet* **401** 577–89
[10] Song J, Gasparrini A, Fischer T, Kejia H and Lu Y 2023 Effect modifications of overhead-view and eye-level urban greenery on heat–mortality associations: small-area analyses using case time series design and different greenery measurements *Environ. Health Perspect.* **131** 097007
[11] Song J, Gasparrini A, Wei Di, Lu Y, Kejia H, Fischer T B and Nieuwenhuijsen M 2024 Do greenspaces really reduce heat health impacts? Evidence for different vegetation types and distance-based greenspace exposure *Environ. Int.* **191** 108950
[12] Wu Y *et al* 2025 Estimating the urban heat-related mortality burden due to greenness: a global modelling study *Lancet Planet. Health* **9** 101235
[13] Achebak H, Masselot P, Ballester J, Gasparrini A and Rey G 2026 Greening mitigates heat-related mortality in Paris *npj Urban Sustainability* **6** 29
[14] Wang S *et al* 2025 Dual impact of global urban overheating on mortality *Nat. Clim. Change* **15** 497–504
[15] Falchetta G, Lohrey S, Souverijns N, Lauwaet D, Schleussner C-F, and Niamir L 2026 Street green space is relevant but not sufficient for adapting to growing urban heat in world cities *Environ. Res. Lett.* Forthcoming; preprint submitted on 10 March, 2026

[16] Pascal M, Goria S, Wagner V'ene, Sabastia M, Guillet A'es, Cordeau E, Mauclair C and Host S 2021 Greening is a promising but likely insufficient adaptation strategy to limit the health impacts of extreme heat *Environ. Int.* **151** 106441
[17] Pascal M *et al* 2024 Analyzing effect modifiers of the temperature-mortality relationship in the Paris region to identify social and environmental levers for more effective adaptation to heat *Health Place* **89** 103325
[18] Monnier R, Personne E, Stella P, de Paula L F, Schalbart P, Roux C and Peuportier B 2026 Balancing positive and negative environmental impacts of urban greening considering future climate: a case study in the Paris region, France *City Environ. Interact.* **29** 100277
[19] Nazish A, Abbas K and Sattar E 2024 Health impact of urban green spaces: a systematic review of heat-related morbidity and mortality *BMJ Open* **14** e081632
[20] Marvuglia A, Koppelaar R and Rugani B 2020 The effect of green roofs on the reduction of mortality due to heatwaves: results from the application of a spatial microsimulation model to four European cities *Ecol. Model.* **438** 109351
[21] Seiferling I, Naik N, Ratti C and Proulx R 2017 Green streets- quantifying and mapping urban trees with street-level imagery and computer vision *Landscape Urban Plan.* **165** 93–101
[22] Zanaga D *et al* 2025 ESA WorldCover 10 m 2021 v200 Sentinel-2 annual composites (2020–2021). Band 1 (p90) used as peak-greenness NDVI at 10 m resolution. CC-BY 4.0. (available at: https://registry.opendata.aws/esa-worldcover-vito-composites/)
[23] Schiavina M, Freire S, and MacManus K 2023 GHS-pop r2023a - GHS population grid multitemporal 1975–2030 (available at: http://data.europa.eu/89h/2ff68a52-5b5b-4a22-8f40-c41da8332cfe)
[24] Falchetta G and Hammad A T 2025 Tracking green space along streets of world cities *Environ. Res.: Infrastruct. Sustain.* **5** 025011
[25] Souverijns N, Lauwaet D, Lejeune Q, Kropf C M, Yeung K L, Nath S and Schleussner C F 2026 100m climate and heat stress data up to 2100 for 142 cities around the globe *Data Brief* **65** 112497
[26] Turner H and Firth D 2023 gnm: generalized nonlinear models R package version 1.1-5 (available at: https://CRAN.R-project.org/package = gnm)
[27] Gasparrini A and Armstrong B 2025 DLNM: distributed lag non-linear models R package version 2.4.10 (available at: https://CRAN.R-project.org/package = dlnm)
[28] Nazarian N *et al* 2022 Integrated assessment of urban overheating impacts on human life *Earth's Future* **10** e2022EF002682
[29] Colaninno N, Basu R, Hosseini M, Alhassan A, Liu L and Sevtsuk A 2025 A sidewalk-level urban heat risk assessment framework using pedestrian mobility and urban microclimate modeling *Environ. Plan. B: Urban Analytics City Sci.* **52** 1071–90
[30] Ibsen P C, Mchale M R, Desouza P, Steinharter L, Green C, Diffendorfer J E and Warziniack T 2026 Moving toward a more human-oriented analysis of urban heat: examining differences of heat exposure intensity at busy commuting locations *Environ. Res.: Health* **4** 015016
[31] Aboudrar-Méda A 2026 Replication materials for: "Urban green space metric choice and weighting matter for assessing cooling benefits for human health" *Github* (available at: https://github.com/ArmandeCMCC/GVIestim)